# Sequential novel use of Moringa oleifera Lam., biochar, and sand to remove turbidity, E. coli, and heavy metals from drinking water

Cleaner Water 2 (2024) 100050

Contents lists available at ScienceDirect

Cleaner Water

journal homepage: www.sciencedirect.com/journal/cleaner-water

# Sequential novel use of *Moringa oleifera* Lam., biochar, and sand to remove turbidity, *E. coli,* and heavy metals from drinking water

Ahsan Shah [a], Arun Arjunan [b,*], Georgina Manning [a], Maryam Batool [c], Julia Zakharova [a], Alisha J. Hawkins [a], Fatima Ajani [a], Ioanna Androulaki [a], Anusha Thumma [d]

[a] Faculty of Science and Engineering, University of Wolverhampton, WV1 1LY, UK
[b] School of Engineering, Computing and Mathematical Sciences, University of Wolverhampton, WV1 1LY, UK
[c] Department of Chemistry, University of Sahiwal, Sahiwal, Pakistan
[d] Department of Pharmaceutical Sciences, College of Pharmacy, Nova Southeastern University, FL, USA

ARTICLE INFO

*Keywords:*
Water purification
Natural coagulants
Carbonised biomass
Suspended solids
Pathogens
Toxic metals

ABSTRACT

This research investigates the individual and combined use of *Moringa oleifera* (MO) Lam., biochar, and sand to remove turbidity, pathogens, and heavy metals from drinking water. Contaminated water was synthetically prepared using kaolin, standard nickel/lead solutions, and *Escherichia coli* (*E. coli*). The optimal dose of MO seed protein, extracted in 1 M NaCl solution, was determined using a jar test flocculator. MO treatment reduced water turbidity from 200 to 4 NTU and achieved a 1–2 log reduction in *E. coli* from an initial count of $1\times10^5$ CFU/ml. Nevertheless, no significant reduction in nickel and lead concentrations was noted. Subsequently, the MO-treated water was passed through a biochar column supported on a sand bed, revealing clear water with 1 NTU turbidity and no trace of *E. coli* counts being detected. The sequential process of using biochar and sand reduced nickel and lead by 97.5 % and 99.3 %, respectively. The physicochemical properties of the treated water met WHO and UK standards for safe drinking water. All experiments were performed in duplicates (n=2; $P < 0.05$). The scalability and economic feasibility of the project, the mechanism of removal of contaminants by MO and biochar, and the study's limitations are also discussed.

## 1. Introduction

Anthropogenic additions of pollutants into water are causing acute and chronic health problems (Alao et al., 2023a; Ayejoto and Egbueri, 2023; Ayejoto et al., 2024, 2023). High water turbidity is one of the indicators of the presence of suspended solids and pathogens like *E. coli* and coliform bacteria, (Tabraiz et al., 2016) which may cause gastro-intestinal infections, pneumonia, neonatal meningitis and sepsis (Shah et al., 2023). Heavy metals like nickel and lead may cause skin allergies, organ damage and cancer if their concentration in water increases threshold limits (Iqbal et al., 2024). Although modern water treatment methods like reverse osmosis, electrodialysis, graphene-based materials and nanomaterials are very effective, they attract high capital costs (Barbosa et al., 2018; Abbas et al., 2023). Moreover, operating and monitoring these methods requires highly skilled labour, which is challenging in underprivileged regions (Zeeshan and Ruhl, 2023). Mediating this issue by using synthetic chemicals like alum may cause other long-term health issues like Alzheimer's (Yavuz and Vaizoğlu, 2013; Doll, 1993; Nkhata, 2002). In this context, the residual aluminium level in the treated water is limited to 0.2 mg/l by the Drinking Water Inspectorate (DWI) UK (Drinking Water Inspectorate (DWI), 2016), 0.05–0.02 mg/l by the Environmental Protection Agency (EPA) USA and 0.2 mg/l by the WHO (World Health Organisation, 2022). The frequent use of these clarifiers by the treatment plants is causing ecological concerns (both toxic and chronic), especially for the fish (Mortula et al., 2009). Furthermore, flocculant chemicals are not readily available in underprivileged regions (Chowdareddy et al., 2023; Dandesa et al., 2023). Consequently, there is an urgent need to establish natural and renewable alternatives to decontaminate drinking water using green chemistry. This is highlighted by the United Nations as a critical area of development, considering the impact it can have on marginalised communities (U. Nations, 2017).

Safe drinking water is defined as water that does not pose significant health risks to consumers. Various regulatory frameworks ensure this

* Correspondence to: Centre for Engineering Innovation and Research (CEIR) School of Engineering, Computing and Mathematical Sciences,University of Wolverhampton, Telford TF2 9NT, United Kingdom.
*E-mail address:* a.arjunan@wlv.ac.uk (A. Arjunan).

https://doi.org/10.1016/j.clwat.2024.100050
Received 3 August 2024; Received in revised form 2 September 2024; Accepted 17 October 2024
Available online 19 October 2024

safety by establishing guidelines and limits for contaminants tailored to each country's specific needs and resources. The World Health Organization (WHO) provides global guidelines on safe contaminant levels, though adherence is voluntary (Binnie Chris Thomas, 2018; Cotruvo, 2017). In the United States, the Safe Drinking Water Act (SDWA), enforced by the Environmental Protection Agency (EPA), sets some of the strictest standards for drinking water safety (U.S.E.P.A. EPA, 2018). Australia's Drinking Water Guidelines (ADWG) address the country's diverse climates by setting region-specific limits under the guidance of the National Health and Medical Research Council (NHMRC) (ADWG, 2024). In Europe, the EU Drinking Water Directive mandates that member states comply with uniform water quality standards (L. and LE, 2020). Similarly, in the UK, the Drinking Water Inspectorate (DWI) monitors and enforces water quality standards across England and Wales to ensure the highest quality of drinking water (D.W.I. dwi, 2019).

From a green chemistry point of view, there is growing literature on *Moringa oleifera* (MO) Lam. seeds and biochar and their potential for water purification. Samia Jahn, in the 1970s, identified the presence of a cationic protein in MO seeds, which was found to be contributing to the coagulation process by attracting negatively charged contaminants and microbes, forming heavier flocs that sink to the bottom. As such, a higher protein concentration can offer significantly improved coagulation efficiency, highlighting its potential for drinking water treatments (Ueda Yamaguchi et al., 2021). Studies by Ndabigengesere et al (Ndabigengesere et al., 1995)., Madsen (Madsen et al., 1987), Okuda et al (Okuda et al., 1999)., Bichi et al (Bichi et al., 2012). and Grabow (Grabow et al., 1985; Wok Grabow et al., 19851985) have also confirmed the potential of MO seeds for water purification.

MO seed protein has an isoelectric potential of 9–11 and a molecular mass ranging from 6 to 16 kg Dalton (kDa) (Amran et al., 2018a). The seed protein offers various functional groups derived from amino acids, the primary constituent of the seed protein. These groups mainly include the amino group (-$NH_2$), carboxylic group (-COOH), hydroxyl group (-OH), amide group (-$CONH_2$), and phenyl group (aromatic ring). These functional groups in MO seeds act as natural clarifiers, reducing water turbidity and other contaminants and rendering their coagulation efficiency comparable to alum (Chowdareddy et al., 2023; Shah et al., 2024a). Furthermore, the macromolecular netty structure of the seed protein itself helps remove pollutants by adsorption and inter-particle bridging (Shabaa et al., 2021). The positively charged coagulant protein can also attract the negatively charged contaminants, removing them through coagulation and sedimentation when the pH of a solution is less than 10 (Saleem and Bachmann, 2019).

Like MO, biochar is another sustainable material extensively explored as a green chemistry alternative for water treatment (Kozyatnyk and Njenga, 2023). Biochar is a carbonaceous material obtained from the pyrolysis of biomass in an oxygen-limited atmosphere at a temperature of 200–1200 °C (Inyang et al., 2016). The raw material required for its synthesis is abundant, and the process is simple and environmentally friendly (Shah et al., 2024a). The process also helps carbon sequestration by avoiding biomass degradation, which otherwise may generate greenhouse gases (Sizmur et al., 2017). High-temperature pyrolysis results in a high surface area, thus improving the adsorption capacity of biochar (Blanco-Canqui, 2019). The pH of biochar is alkaline, ranging from 7.5 to 10, since metals like calcium, magnesium, sodium, and potassium detach from the parent biomass during pyrolysis and accumulate into biochar product (Shakoor et al., 2020). The high porosity, large surface area, macro-morphological structure, and numerous functional groups on the biochar surface make it an excellent adsorbent for removing metals, pathogens, and other impurities (Wang et al., 2019). The removal mechanism can involve adsorption, chemisorption, making chelates, diffusion through pores, and ion exchange (Shah et al., 2024b). Biochar is much cheaper than activated carbon due to the low temperature and energy requirements during pyrolysis (Inyang et al., 2016; Cha et al., 2016; Huggins et al., 2016).

Combining different natural materials that offer a range of properties can be the most efficient way to decontaminate polluted water. For example, the use of sand, along with biochar, has offered improved performance in removing heavy metals and *E. coli*. 3 log removal of *E. coli* was achieved *(*Mohanty et al., 2014*)*. Lau et al (Lau et al., 2017). suggested modifying biochar with sulfuric acid to enhance the removal of *E. coli* from stormwater. The acid-modified biochar could remove up to 98 % of *E. coli*. The addition of alum and activated carbon to MO was explored by De Paula et al., 90 % removal of turbidity could be achieved (De Paula et al., 2014). Sera et al (Sera et al., 2021)., studied removing heavy metals from water using MO powder and activated carbon. A high percentage removal of As, Pb and Cd was obtained. Kozyatnyk and Njenga (Kozyatnyk and Njenga, 2023) used a combination of MO and biochar to study the removal of multiple heavy metals, including Cr, Co, Zn, Ni, and Pb. A 5–58 % removal was reported. Most of these studies involved expensive technological protocols and synthetic agents, which fall outside the scope of green chemistry from a practical point of view.

There is a significant gap in the literature regarding the use of cost-effective and simple procedures to combine natural materials for the treatment of drinking water, which this study aims to provide. This is the first study focusing on the combined, sequential use of *Moringa oleifera*, biochar and sand to treat drinking water. The primary objective here is to evaluate the effectiveness of MO, sand, and biochar in removing turbidity, *E. coli*, and heavy metals from contaminated water, both individually and in combination. The hypothesis posits that (a) increasing the dose of MO protein and the length of the biochar column will enhance contaminant removal efficiency, and (b) the sequential use of MO and biochar will improve the water quality. To substantiate the efficiency of the devised system, the treated water was checked for its physicochemical properties to ensure that it meets drinking water criteria set by the World Health Organisation (WHO) and UK standards. Notably, all materials used to remove contaminants in this study were food-grade. Sewage sludge-derived biochar (SSB), which offers dual advantages by managing hazardous waste and treating contaminated water, was the biochar of choice. The adoption of natural resources to provide potable water is being advocated by the United Nations and is linked to its Sustainable Development Goals SDG 6 and SDG 3 (UNDP, 2023).

## 2. Methodology

### 2.1. Materials

Sun-dried MO seeds aged (post-drying) six months were procured from a farmer in Lahore, Pakistan. The UK Biochar Research Centre at the University of Edinburgh provided sewage sludge-derived biochar (SSB) pyrolysed at 700 ℃. This research used fine sand of 0.2–0.5 mm grain size purchased from Amazon and China clay (Kaolin) acquired from Trusleaf Ltd, UK. The University of Wolverhampton provided *E. coli* k12 for microbial studies, initially sourced from NCIMB Ltd. Aberdeen, UK.

Sodium chloride (analytical grade) used to extract the MO protein was sourced from Fischer Scientific, UK. Tap water and deionised water were obtained from the University's microbiology projects laboratory. The standard metal solutions were prepared using lead nitrate (99 %) and nickel sulphate (99 %) metal salts bought from Fisher Scientific Ltd. and Scientific & Chemical Supplies Ltd. UK, respectively. Table 1 and

**Table 1**
Physicochemical characteristics of tap and distilled water used for experiments.

| Parameter | Distilled water | Tap water |
|---|---|---|
| pH | 6.8 ± 0.2 | 7.6 ± 0.2 |
| TDS (ppm) | 1.0 – 2.0 | 248–255 |
| Hardness (Clarke) | trace | 13.10 |
| Conductivity (μs/cm) | 2–3 | 501 |
| Turbidity (NTU) | 0.10 | 0.5 |

**Table 2**
Physicochemical properties of SSB adsorbent. Here, Ms/cm stands for milli Siemens per centimetre.

| Property | Value |
|---|---|
| pH | 9.60 |
| Electric conductivity | 133.4 mS/cm |
| C stability | 96.44 % |
| Total ash | 63.91 wt% |
| Moisture | 1.69 wt% |
| Adsorption capacity | 3.02–2.51 mg/g (Shah et al., 2024b). |

Table 2 report the physicochemical properties of the tap and distilled water used and the sewage sludge biochar, respectively.

### 2.2. Preparation of reagents

#### 2.2.1. Synthetic turbidity solution

3 g kaolin was mixed with 5 L tap water and left overnight for the hydrolysis process to complete. The mixture was stirred for 30 minutes at 500 rpm using a Stuart magnetic stirrer, resulting in a stock solution of approximately 1000 NTU turbidity, which was subsequently diluted as required for various experiments.

#### 2.2.2. Standard heavy metal solutions

Standard 1000 mg/L solutions of nickel and lead were prepared from hydrated nickel sulphate ($NiSO_4.6H_2O$) and lead nitrate ($Pb(NO_3)_2$) salts by dissolving stoichiometric amounts in deionised water. Heavy metal solutions of desired concentrations for various experiments were created through further dilutions as desired.

#### 2.2.3. Preparation and characterisation of biochar

SSB was sieved to obtain a particle size (PS) range of 0.4–0.8 mm, the same as that of MO seeds. The sieved biochar was washed with warm water at 40 °C and then deionised water to remove any physical contaminants on its surface. It was oven-dried at 112 °C till it reached a constant weight. The resulting biochar was used in the column to remove pollutants from the synthetically made turbid water. The sand was used without any treatment as a supportive adsorbent bed.

Each adsorbent (SSB, MO, and sand) was characterised through five different analytical techniques, namely (i) FTIR (Bruker Alpha 1) for determining the functional groups (Wei et al., 2018), (ii) SEM (Zeiss EVO 50 kit) for the morphological study (Muneer et al., 2021), (iii) XRD (Panalytical Empyrean equipment) for crystallographic analysis (Azhar-ul-Haq et al., 2022), (iv) X-ray fluorescence screening (Panalytical Epsilon 3) kit for the elemental analysis (Ghzal et al., 2023).

#### 2.2.4. Extraction of MO seed protein

Good-quality seeds were handpicked and manually deshelled before grinding into a fine powder using a stainless-steel pestle and mortar. The powder obtained was sieved to achieve a particle size range of 0.4–0.8 mm. The sieved seed powder was dissolved in a freshly prepared 1 M NaCl solution (2 % w/v) to extract the coagulant seed protein. The mass was stirred for 3 minutes using a Stuart magnetic stirrer at 240 rpm. After 1 h, it was filtered using a cotton cloth. The filtrate, the *Moringa oleifera* seed protein extract (MOSE), was used in experiments at varying calculated dose rates.

### 2.3. Dose optimisation of MOSE

A turbidity solution of 200 NTU made from the stock solution was taken into six glass beakers. 10 mg/L nickel, 10 mg/L lead and $1\times10^5$ colony-forming units (CFU)/ml of *E. coli* were added into each beaker. Varying doses of MOSE were added to each beaker and placed in a Stuart flocculator SW6 equipped with six rotators. The beakers were flocculated by flash mixing for 2 minutes at 130 rpm to achieve a thorough mixing, followed by a slow mixing for 15 minutes at 36 rpm to aid the flocculation. The control sample contained the same concentration of synthetic contaminants without featuring any MOSE. The flocculated beakers were allowed to settle, and the turbidity of the solution in each beaker, including the control sample, was measured after 1, 1.5, 2 and 2.5 h. The *E. coli* concentrations were measured every hour until clear water of less than 5 NTU was obtained. The *E. coli* growth was monitored again in each beaker to check for any regrowth of the pathogens after 24 h. The optimum dose was the MO dosage that offered minimum turbidity and *E. coli* growth. The methodology adopted here is consistent with previous literature (Shabaa et al., 2021; Delelegn et al., 2018).

### 2.4. Physicochemical characterisation

The residual turbidity (RT) of water was measured using a calibrated Lovibond conductivity photometer model TB211IR, and the percentage turbidity removal (% $R_T$) was calculated using Eq. (1) (Shabaa et al., 2021; Shamsnejati et al., 2015a):

$$\%\quad R_T = \frac{T_i - T_f}{T_i} \times 100 \tag{1}$$

Where $T_i$ and $T_f$ represent the turbidity (NTU) of the samples before and after flocculation, respectively. A calibrated Hanna pH meter model pH 20 was used to measure the pH of the samples. A Jenway 4510 model conductivity meter and a Hanna's TDS meter were used to measure the conductivity and the concentration of total solids in the beakers. Weight measurements were performed using Sartorius Secura portable precision balance. Agilent Technologies 5100 inductively coupled plasma–optical emission spectroscopy (ICP-OES) was used to measure the residual concentration of elements like nickel (Ni), lead (Pb), calcium (Ca), magnesium (Mg), iron (Fe) and silicon (Si). The dissolved oxygen (DO) of the samples was measured using a WTW 3410 m. All the kits passed PAT (portable appliance test) and were calibrated before conducting the relevant tests.

### 2.5. Microbial load characterisation

Nutrient broth containing *E. coli* k12 was shaken for 12 h at 37 °C using a Thermo-scientific MAXQ 8000 shaker to promote aerobic conditions for bacterial growth. All the accessories used in the experiment, including the pestle and mortar, sieves, beakers, and micropipette tips, were autoclaved for 20 minutes at 15 psi and 121 °C in a Prioclave autoclave. Each beaker was seeded with *E. coli* at $1\times10^5$ CFU/ml and flocculated using a jar test flocculator. After 1 and 2 h, a 20 µl sample was taken from each beaker and incubated on agar plates at 37 °C for 12 h. The gram staining method was used to identify the type of microbial growth. The concentration of *E. coli* in each beaker, including the control sample, was determined using Eq. (2):

$$N = \quad n_c \times d_f \times p_f \tag{2}$$

Where N is the concentration of $E.coli\ (CFU/ml)$, $n_c$ represents the number of colonies counted, $d_f$ is the dilution factor, and $p_f$ is the plating factor. The method adopted was similar to the ones reported in studies (Delelegn et al., 2018; Vega Andrade et al., 2021). All experiments were performed in duplicates (n = 2).

### 2.6. Statistical analysis

All experiments were conducted in duplicate (n=2) to enhance the reliability of the study findings (average of determinations ± standard deviation). An ANOVA test was then applied to determine if there were statistically significant differences between the results obtained from the duplicate experiments. The P value was $< 0.05$. By performing experiments in duplicate, we aimed to minimise the potential impact of random errors.

## 3. Results and discussion

### 3.1. Functional groups

FTIR analysis of the biochar, MO and sand was performed within a 4000–500 $cm^{-1}$ range at an instrumental resolution of 4 $cm^{-1}$ with 32 scans per sample. The study results shown in Fig. 1 revealed the presence of various organic and inorganic functionalities in each studied adsorbent. Numerous small peaks from 3500 to 3300 $cm^{-1}$ in raw biochar before metal adsorption correspond to the stretching vibrations of the hydroxyl groups of different organic and inorganic compounds. Further, the stretching vibrations of -C≡C- and -C≡N bonds appeared within the 2300–1900 $cm^{-1}$ range. Small peaks within 1550–1300 $cm^{-1}$ correspond to the stretching vibrations of carbon-oxygen (C═O) bonds of groups like ketonic, ester, carboxylic, and anhydrides. Small peaks obtained at 1579.18 $cm^{-1}$ and peak obtained at 999.74 $cm^{-1}$ correspond to the stretching vibrations of the -Si-O bonds in aromatic compounds and the -C-O vibrations, respectively (Mandu et al., 2015).

However, after the adsorption of Pb and Ni on biochar, the small peaks within the range 1900–2300 $cm^{-1}$ disappeared, thus confirming the involvement of -C═O, -C≡C- and -C≡N bonds in the adsorption of metals. There was a shift in the minor peaks of the O-H group (3500–3300 $cm^{-1}$) and C═O bonds (1650–1300 $cm^{-1}$) after metal adsorption, indicating the involvement of hydroxyl and carboxyl groups in the adsorption of Pb and Ni. Post-adsorption of metals, there was a shift in the peak intensity at 999.74 $cm^{-1}$, confirming the involvement of -Si-O functional groups in adsorption. Additionally, the variation in peaks within the range 3500–3300 $cm^{-1}$ reveals the possible involvement of hydroxyl groups (Azhar-ul-Haq et al., 2022; Ghzal et al., 2023).

Fig. 1 further reveals the presence of different functionalities of MO as stretching vibrations of O-H and N-H (amide groups) obtained at 3400 $cm^{-1}$ having a broadband peak. These vibrations of the O-H and N-H groups reveal the presence of protein and fatty acid structures as the main constituents of *Moringa oleifera*. Further, symmetrical and asymmetrical stretching vibrations of the C-H bond (of the $CH_2$ group of fatty acid) and -C═O bonds (of fatty acid and protein) were shown at 2921.70 $cm^{-1}$ and 2852.33 $cm^{-1}$ and in the regions between 1800 and 1600 $cm^{-1}$ respectively. Bands that appear at 1744.45 $cm^{-1}$ and 1644.47 $cm^{-1}$ are associated with fatty acids, while the amide group of protein and C-N stretching or N-H deformation results in peaks at 1579.18 $cm^{-1}$ and 1540.42 $cm^{-1}$, respectively. Overall, the results of FTIR confirm the presence of protein structure in MO seeds (Hoa and Hue, 2018; Gaikwad and Munavalli, 2019). For sand, the FTIR spectrum indicates adsorption bands at 681.45 $cm^{-1}$ and 791.63 $cm^{-1}$, revealing the presence of quartz mineral as the main composition. The peaks obtained at 1093.59 $cm^{-1}$ and 2160.67 $cm^{-1}$ correspond to symmetric vibrations of the Si-O group and the -C═O stretch bending vibration (Amran et al., 2022).

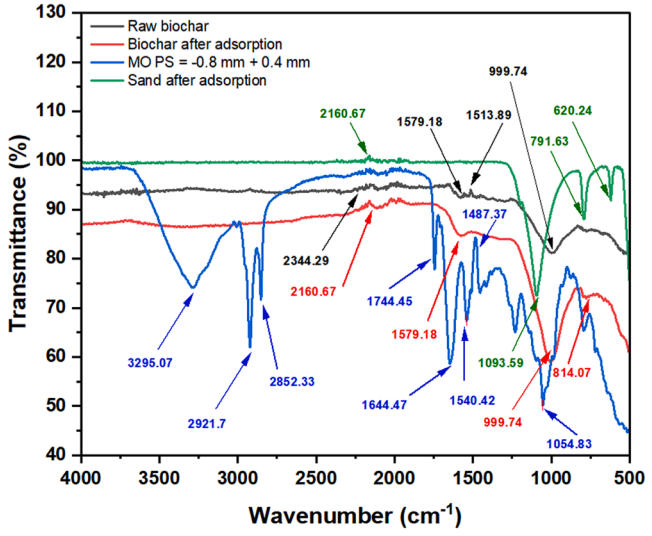


**Fig. 1.** FTIR analysis comparing raw biochar, biochar after adsorption, raw *Moringa oleifera* and sand after contaminant adsorption highlighting the involvement of various functional groups, such as -O-H, -C-O and -N-H, in the adsorption process.

Significant changes in the peak intensity and position of key functional groups, including hydroxyl (-OH), carbonyl (-C═O), carboxyl (-COOH), and amine (-NH) groups, were observed for each studied material. These variations strongly suggest the direct involvement of these functional groups in the adsorption process. The observed changes likely indicate the formation of new bonds (mainly electrostatic interactions, H-bonds) between the adsorbate molecules and the functional groups on the adsorbent surface, leading to the removal of contaminants from the solution (Azhar-ul-Haq et al., 2022; Kwabena Ntibrey et al., 2020). It is worth mentioning that FTIR analysis of MO post-treatment was technically not feasible for this study. The reason is that the high dilution of the seed protein as used for coagulation, prevents characterisation. Unlike the powder, the solution, especially at a high dilution, obscures the revelation of its actual surface characteristics (Shah et al., 2024c).

### 3.2. Morphological study

SEM analysis was carried out on the adsorbents, before and after the adsorption of Pb and Ni to morphologically characterise the adsorbents. Before sorption, as revealed in Fig. 2, the surface of the biochar (Fig. 2a-b), MO (Fig. 2e-f), and sand (Fig. 2g-h) was highly rough, with numerous cavities present on their surface. These active sites play a crucial role in adsorption, serving as the binding points for the adsorption of metal ions on the surface. Following the adsorption process, the morphological characteristics of each studied adsorbent are shown in Figs. 2b-c and 2i-j. These characteristics reveal the variation in the surface texture from a highly rough and heterogeneous structure to a somewhat homogeneous one. These results suggest that the studied adsorbents have effectively captured and adsorbed the metal ions from the solution (Saleem et al., 2020; Li et al., 2017).

Biochar is characterised by its large surface area and interconnected pore network. As shown in Fig. 2a-b, this morphology acts as vacant sites for the adsorption of various contaminants, including heavy metals. As adsorption occurs, the surface morphology of biochar evolves with the formation of adsorbate-biochar complexes. These alterations influence the surface area and pore size distribution, as shown in Fig. 2c-d. Studies by Lehmann have highlighted the significant role of biochar morphology in governing adsorption mechanisms, emphasising the importance of understanding morphological changes for adsorption applications (Johannes Lehmann, 2015).

Fig. 2e-f shows the SEM analysis of *Moringa oleifera* powder within the 0.4–0.8 mm particle size range, revealing features of its surface morphology, such as the shape, texture, and structural features of the particles. The MO powder particles can be seen to exhibit a heterogeneous morphology characterised by irregular shapes and sizes. Furthermore, the SEM analysis reveals variations in particle shape and size distribution within the 0.4–0.8 mm range. Some particles are more spherical or ellipsoidal, while others appear more irregular and angular. This heterogeneity in particle morphology may result from differences in seed characteristics, processing conditions, and particle aggregation during powder formation (Saleem et al., 2020).

Regarding sand, the SEM micrographs reveal its natural morphology characterised by its irregular shapes, rough surfaces, and heterogeneous composition, as shown in Fig. 2g-h. Sand grains typically exhibit various sizes and shapes, with surface features such as pits, cracks, and mineral coatings. The porous nature of sand provides numerous sites for the adsorption of heavy metals, including surface adsorption, ion exchange, and precipitation. Following the adsorption of heavy metals, Fig. 2i-j

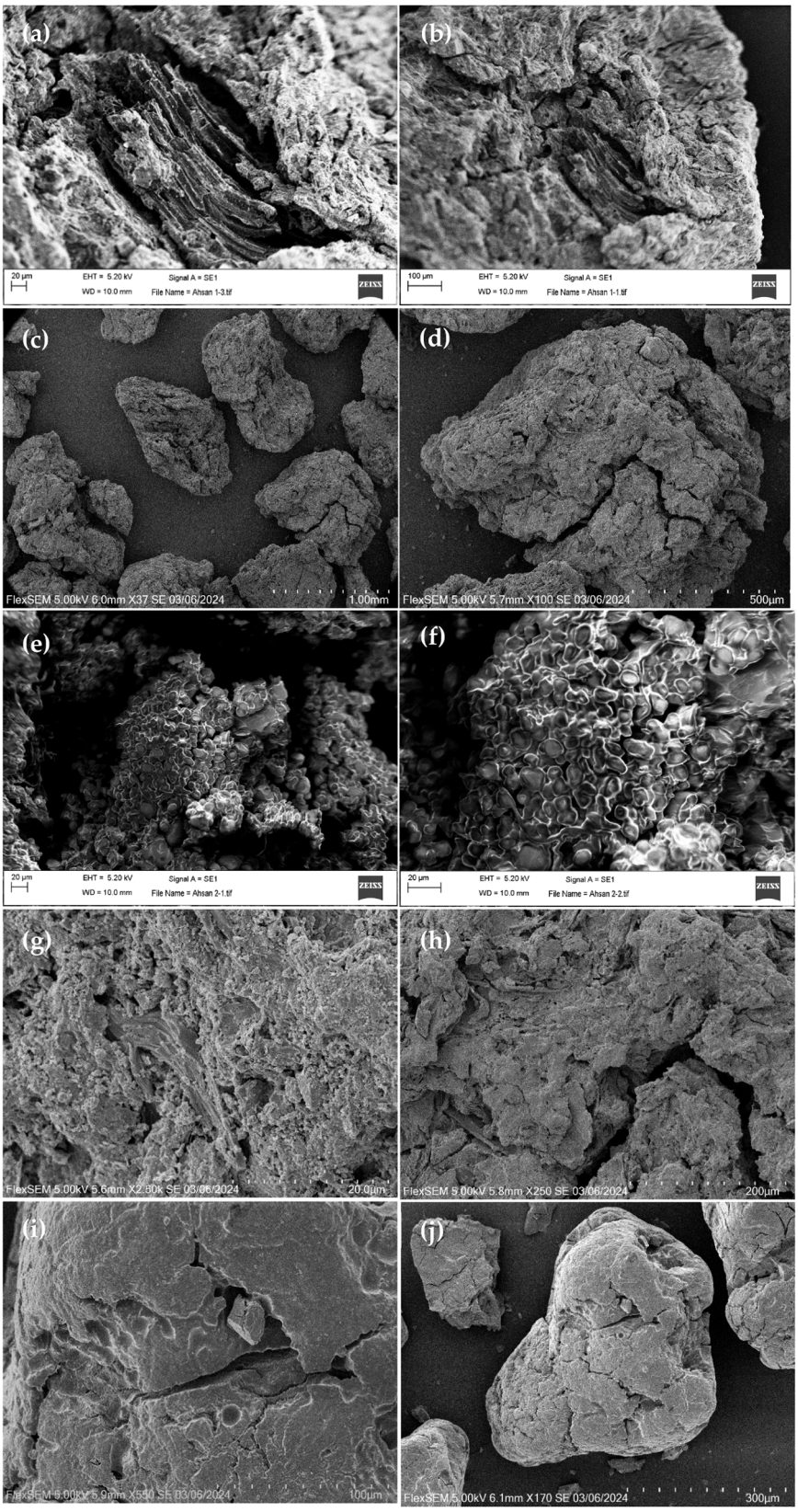


**Fig. 2.** Scanning electron micrograph of all the three adsorbents showing (a-b) biochar before adsorption at different magnifications, (c-d) biochar at different magnifications after adsorption, (e-f) MO at different magnifications, (g-h) sand at different magnifications before adsorption and (i-j) sand after adsorption of contaminants. The study revealed the heterogeneous surface of each studied material, favouring the adsorption process.

shows notable changes in the surface morphology and structure of sand particles. SEM data also shows clusters immobilised on the sand surface, indicating successful adsorption and removal of heavy metals from the solution. Overall, the qualitative analysis of the SEM images revealed a significant decrease in the particle size distribution of adsorbents after adsorption. This suggests the metal ions may have filled the smaller pores and cavities on the biochar surface (Muneer et al., 2021; Azhar-ul-Haq et al., 2022).

### 3.3. Crystallographic analysis

Results of the XRD analysis of biochar, MO and sand are revealed in Fig. 3, where the metal adsorption peaks for biochar (Fig. 3a) appear at an angle of 18–28° representing the crystal plane index C (002), signifying the parallel and azimuthal alignment of aromatic and carbonised lamellae. In addition, the peaks at 40–46° angle represent crystal plane index C (100) corresponding to the condensed aromatic carbonised planes. The presence of $CaCO_3$ (calcite), $SiO_2$ (quartz), CaO (lime), Ca $(OH)_2$ and $Al_2O_3$ (alumina) was confirmed by the peaks obtained at an angle of 43° (JCPDS card no. 05-0586), 68–72° (JCPDS card no. 46-1045), 41° (JCPDS Card no. 011-1160), 60° (JCPDS card no. 01-073-5492) and 83° (JCPDS Card no. 11-0517), respectively (Shah et al., 2024a; Muneer et al., 2021).

For sand, as shown in Fig. 3b, a high degree of crystallinity was observed, as validated by the narrow peaks obtained. Some quartz phases were also found in the highest relative intensities, with some impurities such as $Al_2O_3$, $Fe_2O_3$, and $ZrO_2$ being present in minor phases (Su et al., 2021). This crystalline material exhibited excellent adsorption properties, which can be attributed to its unique crystallographic characteristics. The specific crystal structure and surface morphology provided numerous adsorption sites and facilitated the diffusion of adsorbates.

The presence of functional groups within the crystal lattice further enhanced the material's ability to interact with and adsorb contaminants. These adsorption sites can interact with adsorbate molecules through various mechanisms, such as physical adsorption (weak van der Waals forces), chemisorption (strong chemical bonding), or ion exchange. Regarding MO, the XRD data (Fig. 3c) reveals a high quantity of proteins in the material composition at the particle size studied (0.4–0.8 mm). The de-husked MO seeds appear amorphous, informed by a partially resolved X-ray pattern, which is favourable for adsorption.

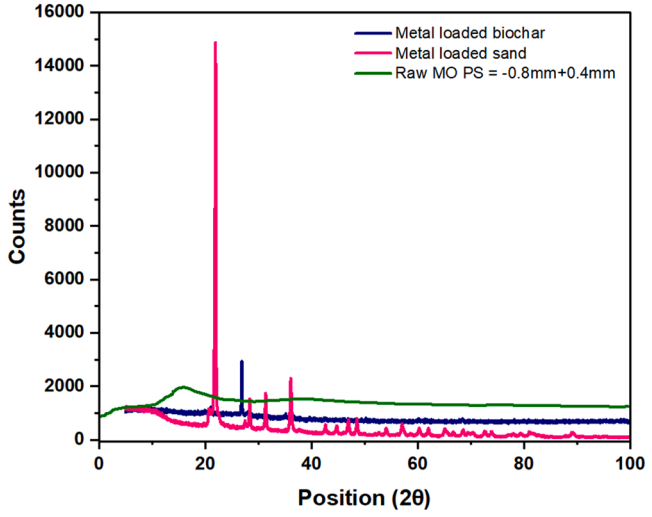


**Fig. 3.** XRD analysis revealing the crystallographic characteristics of (a) post-adsorption biochar, (b) post-adsorption sand and (c) raw MO. The study revealed the presence of different aromatic compounds and various heterogeneous substances, including proteins, lipids, and minor proportions of carbohydrates and ash.

The peak at 2θ approximates 20, corresponding to the diffraction of the amorphous constituent protein of MO. The XRD data also confirmed various heterogeneous substances, including proteins, lipids, and minor proportions of carbohydrates and ash (Shah et al., 2024c; Saleem et al., 2020).

### 3.4. Elemental composition

The X-ray fluorescence screening (XRF) was performed for the biochar after the adsorption of the contaminants. It revealed the presence of different cationic, anionic, and neutral elements in SSB, having different percentage compositions, as summarised in Table 3. Before metal adsorption, biochar was mainly composed of carbon C (29.55 %), hydrogen H (0.83 %), nitrogen N (3.79 %), oxygen O (2.75 %), silica Si (2.019 %), phosphorous P (1.074 %), and many other trace elements. The total ash content of the SSB is 63.91 % (UK Biochar Research Centre and Welcome to the UKBRC,). No change in the composition of these elements was observed after adsorption. While the elemental composition of most elements remained unchanged after adsorption, a significant increase in lead and nickel concentrations was observed. This suggests that the SSB selectively adsorbed these heavy metals, likely due to interactions between the metals and functional groups on the biochar surface. Further analysis, such as FTIR, helps to identify the specific functional groups involved in the adsorption process, which is the study's main objective.

### 3.5. Performance of MO Lam

#### 3.5.1. Selection of contaminants

The water to be treated was synthetically prepared to replicate heavily contaminated water. A turbid solution of 200 NTU was obtained by adding kaolin clay to tap water and thoroughly mixing it. Turbidity is the measure of suspended solids (SS) present in a solution, and its allowable level in drinking water is up to 5 NTU (World Health Organisation, 2022). Contaminants like algae, clay, silt, and some other organic and inorganic substances may attach to the SS. Similarly, pathogens can hide inside the clay particles, requiring an additional dose of bactericides or clarifiers (Hoa and Hue, 2018). Lead and nickel were added to this solution to study the removal of these heavy metals by diluting the stock solutions of lead nitrate and nickel sulphate.

Heavy metals are toxic contaminants that persist in the environment and pollute the ecosystems (Ayeni et al., 2022). Lead is number 2 on the ATSDR list of toxic substances, with a permissible limit of 10 μg/l or 0.01 mg/l (Baskaran and Abraham, 2022). Exposure over this limit can damage kidneys and cause neurological effects in pregnant mothers and infants. Similarly, nickel, limited at 0.07 mg/l (Babakhani and Sartaj,

**Table 3**
XRF analysis of biochar (SSB) before and after adsorption revealed a significant increase in the percentages of Pb and Ni. These findings strongly suggest the successful adsorption of these metals onto the surface of the biochar.

| Element | SSB composition | |
|---|---|---|
| | Before adsorption | After adsorption |
| C | 29.55 wt% | 29.55 wt% |
| H | 0.83 wt% | 0.83 wt% |
| O | 2.75 wt% | 2.75 wt% |
| N | 3.79 wt% | 3.79 wt% |
| Si | 2.02 wt% | 2.02 wt% |
| P | 1.07 wt% | 1.07 wt% |
| Mg | 500.19 mg/l | 530.23 mg/l |
| As | 0.78 mg/l | 0.78 mg/l |
| Cr | 284.10 mg/l | 284.14 mg/l |
| Co | 13. 14 mg/l | 13.19 mg/l |
| Pb | 196.68 mg/l | 206.60 mg/l |
| Ni | 70.52 mg/l | 80.24 mg/l |
| Se | 1.59 mg/l | 2.37 mg/l |
| Zn | 900.51 mg/l | g/l |

2023), can result in skin irritations and damage the stomach, lungs and kidneys. To characterise MO's performance, lead and nickel were added at a concentration of 10 mg/l. To study the reduction of pathogens, *Escherichia coli (E. coli)* were added to the synthetic mixture solution at a high concentration of $1\times10^{5}$ CFU/ml, an approach consistent with the literature (Grabow et al., 1985; Delelegn et al., 2018). The reason for this selection was that the presence of *E. coli* is indicative that the water may have faecal contamination directly or indirectly, such as through a leaking sewerage pipe. Several water-borne diseases, including diarrhoea, typhoid, nausea, cramps and headaches, are caused by *E. coli*. The maximum acceptable limit of *E. coli* in drinking water is 100 MPN/ml (MPN stands for most probable number) (World Health Organisation, 2022).

### 3.5.2. Selection of extractant for seed protein

The MO seed protein was extracted in 1 M NaCl instead of water. According to researchers like Okuda et al (Johannes Lehmann, 2015). and Magersa et al (Su et al., 2021)., both water and salt-extracted solutions contain protein and polysaccharides. However, the ionic strength of salt-extracted MO protein is much higher than water-extracted variants. This increases the solubility of the seed protein, offering improved coagulation at lower doses.

### 3.5.3. Reduction in turbidity

The reduction in turbidity of synthetically contaminated water by applying varying doses of MO salt extracts is summarised in Table 4. The residual turbidity measurement for varying MO doses and treatment times are shown in Fig. 4. MO doses ranged from 25 to 200 mg/l, and the water samples were taken at various time intervals. Initially, after one hour, only the 50 mg/l dose of MO could achieve a turbidity level close to 5 NTU. This reduction in water turbidity can be attributed to the ongoing process of floc formation and their settling, which remained incomplete within this timeframe for the other doses. However, as time progressed, notably after two hours, doses of 50, 75, and 100 mg/l significantly reduced turbidity levels below 5 NTU. This turbidity value aligns with WHO standards for drinking water turbidity (World Health Organisation, 2022). The enhancement in turbidity reduction over time suggests the continued effectiveness of MO salt extracts in clarifying water.

Fig. 4 outlines the residual turbidity of the solutions at different MO doses, with an initial turbidity of 200 NTU. This indicates a dose-response relationship, where higher doses of MO extract led to a more effective reduction in turbidity levels. However, excessively high doses, such as 200 mg/l, do not necessarily yield proportionally more significant decreases and may even exhibit diminishing returns. The study's outcome rejects hypothesis "a" that increasing the dose of MO seed protein increases the coagulation efficiency. This suggests an optimal dosage range for MO salt extracts in water clarification applications. Furthermore, the time-dependence aspect of turbidity reduction highlights the importance of allowing adequate contact time for the clarification process to occur effectively. While significant reductions can be observed within two hours, further improvements continue to manifest over a 24 h period, indicating the persistence and efficacy of MO salt extracts in water treatment applications.

**Table 4**
Residual turbidity of the solution at different doses of MO (Initial turbidity 200 NTU). Experiments were performed in duplicate (n=2). Values are given as average ± standard deviation (S.D.) with P value <0.05.

| 1 M NaCl extracted MO dose mg/l | Residual turbidity (NTU) | | | | |
|---|---|---|---|---|---|
| | 1 h | 1.5 h | 2 h | 2.5 h | 24 h |
| 25 | 10.2 ±0.223 | 6.67 ±0.226 | 5.59 ±0.218 | 4.89 ±0.226 | 2.35 ±0.321 |
| 50 | 6.68 ±0.263 | 3.68 ±0.231 | 2.5 ±0.323 | 1.72 ±0.123 | 1.86 ±0.214 |
| 75 | 10.2 ±0.341 | 7.31 ±0.322 | 4.28 ±0.242 | 3.45 ±0.231 | 1.5 ±0.132 |
| 100 | 16.5 ±0.422 | 6.42 ±0.312 | 6.33 ±0.114 | 4.18 ±0.122 | 2.31 ±0.144 |
| 200 | 26.9 ±0.223 | 16.8 ±0.189 | 10.5 ±0.213 | 10 ±0.412 | 5.59 ±0.323 |

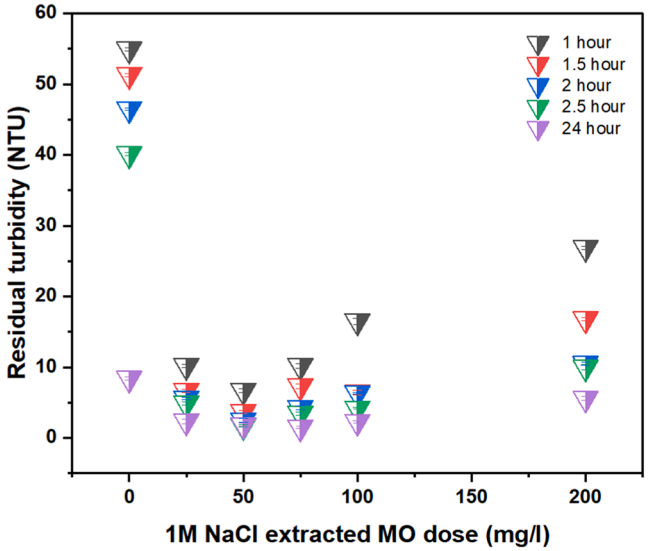


**Fig. 4.** Residual turbidity of the contaminated water treated with different doses of MO after 1, 1.5, 2, 2.5, and 24 h.

### 3.5.4. Reduction in the concentration of Ni and Pb

Table 3 summarises the reductions in nickel and lead concentrations achieved through the application of various doses of MO after 2 h of flocculation. MO demonstrated notable effectiveness in lead removal, as indicated by the considerable reduction in lead concentration across all doses compared to the control sample. However, the removal of nickel appears to be less efficient, with relatively smaller reductions observed across the different MO doses. Table 5 highlights a dose-dependent relationship between MO dose and the removal of heavy metals. As the dose of MO increases from 25 to 200 mg/l, there is a general trend of improved metal removal, with lower concentrations of both nickel and lead observed. This suggests that higher doses of MO have a greater capacity to facilitate the coagulation and subsequent removal of heavy metals from water samples.

However, despite the increase in metal removal with higher MO doses, none of the doses evaluated in the study met the drinking water standard, particularly concerning residual nickel concentrations. The experiment demonstrated that the data did not support the hypothesis "a". Therefore, it was rejected. Overall, Table 5 underscores the potential of MO as a viable option for heavy metal remediation in contaminated water. However, it also highlights the need for continued research and development to enhance its efficacy and ensure compliance with regulatory standards for safe drinking water.

### 3.5.5. Reduction in E. coli

To investigate the efficacy of reducing *E. coli* levels, samples were collected from the beakers at 1 h and 2 h intervals. No further sampling for *E. coli* was considered after the 2 h mark due to achieving clear water within this time frame. Subsequent sampling after 24 h aimed to assess any potential regrowth of *E. coli*. Table 6 summarises the reduction in *E. coli* concentrations across varying doses of salt-extracted coagulant protein.

Analysing the data as shown in Fig. 5, significant reductions in pathogenic growth were observed at MO doses of 50 mg/l (93 %), 75 mg/l (97.5 %), and 100 mg/l (99.6 %) following the 1 h mark. Additional decreases in bacterial counts were recorded after 2 h with

**Table 5**
Reduction in the concentration of Ni and Pb by different doses of MO, 2 h post flocculation.

| Heavy metals | Contaminated water | Control sample | MO 25 mg/l | MO 50 mg/l | MO 75 mg/l | MO 100 mg/l | MO 200 mg/l |
|---|---|---|---|---|---|---|---|
| Ni (mg/l) | 10 | 4.78 | 2.49 | 2.55 | 2.52 | 2.44 | 2.40 |
| Pb (mg/l) | 10 | 3.02 | 0.31 | 0.58 | 0.19 | 0.17 | 0.15 |

**Table 6**
Residual concentrations of *E. coli* at different doses of MO after 1 h and 2 h. Experiments were performed in duplicate (n=2). Values are given as average ± standard deviation (S.D.) with P value <0.05.

| 1 M NaCl extracted MO dose | Residual log *E. coli* (CFU/ml) | |
|---|---|---|
| (mg/l) | 1 h | 2 h |
| 0 | 4.556±0.121 | 3.361±0.311 |
| 25 | 4.146±0.231 | 2.301±0.298 |
| 50 | 3.845±0.224 | 2.602±0.321 |
| 75 | 2.397±0.132 | 2.176±0.214 |
| 100 | 3.531±0.241 | 2.397±0.112 |
| 200 | 4.021±0.126 | 2.778±0.213 |

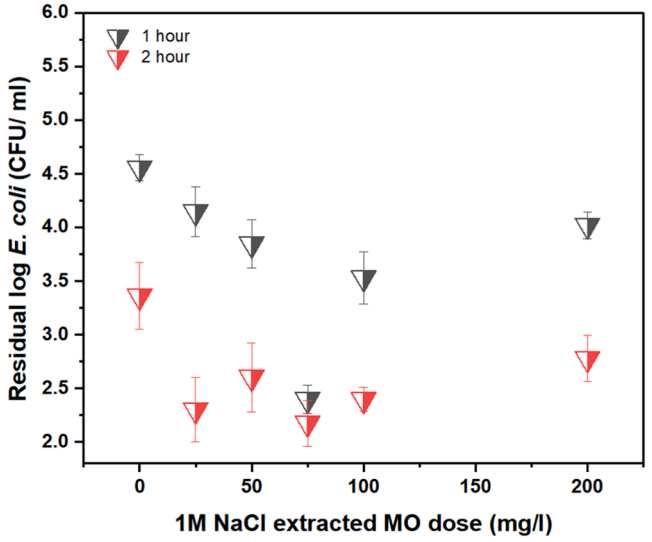


**Fig. 5.** Residual concentration of *E. coli* at different doses of MO after 1 hour and 2 hours.

coagulant doses of 25 mg/l (99.8 %), 50 mg/l (99.6 %), 75 mg/l (99.95 %), and 100 mg/l (99.75 %). Despite these reductions, none of the coagulant proteins completely eradicated *E. coli*, which fell below the WHO recommended standard.

Residual *E. coli* concentrations at different MO doses and time points, as listed in Table 4, highlight the effectiveness of the coagulant in reducing bacterial counts. The inclusion of statistical analysis enhances the reliability of the findings, reinforcing the significance of the observed reductions. Additionally, the results after 2 h show the reduced *E. coli* levels over longer periods post-coagulation.

Table 7 summarises the bacterial growth following 24 h of flocculation with MO protein extracts. Overall, a substantial increase in *E. coli* levels was observed when the beakers were not covered. It could potentially be attributed to the organic nature of MO seed protein, which might attract pathogens over time if the containers are not adequately covered. Subsequent experiments explored that covering the beakers using stretch bands led to no considerable additional growth of *E. coli.* Consequently, keeping the containers properly covered and consuming the treated water within 24 h can be considered the best practice to reduce the risk of bacterial re-growth (Jahn, 1986).

**Table 7**
Residual log *E. coli* at different doses of MO salt-extracted protein after 24 h of flocculation for both covered beakers and beakers without cover. Values are given as average ± standard deviation (S.D.) with a P value <0.05 (n=2).

| 1 M NaCl extracted MO dose | Residual log *E. coli* (CFU/ml) | |
|---|---|---|
| (mg/l) | Not covered | Covered |
| 0 | 12.56±0.211 | 9.61±0.121 |
| 25 | 12.32±0.312 | 7.82±0.169 |
| 50 | 9.97±0.126 | 6.55±0.323 |
| 75 | 9.79±0.241 | 6.47±0.241 |
| 100 | 9.47±0.221 | 5.01±0.311 |
| 200 | 9.21±0.234 | 7.13±0.123 |

Fig. 6 provides a comprehensive comparison of residual *E. coli* levels at different doses of salt-extracted MO protein after 24 h of flocculation, considering both covered and open container conditions. The data here emphasises the importance of considering post-treatment handling procedures in water purification protocols. By addressing factors such as container covering and timely consumption of treated water, practitioners can enhance the effectiveness of MO protein-based flocculation methods in maintaining water safety.

### 3.6. Combined sand and biochar treatment

#### 3.6.1. Purification outcomes and water quality

The combined sand and biochar treatment method was assessed for its efficacy in purifying water, considering various parameters such as turbidity, heavy metals, and *E. coli* reductions. Results were compared against established water quality standards, including pH, turbidity, *E. coli* levels, and concentrations of metals like Ni, Pb, and Fe. Water parameter limits recommended by WHO include turbidity ≤5 NTU, *E. coli* 0/100 ml, Ni ≤0.07 mg/l, and Pb ≤0.01 mg/l. UK standards specify pH 6.5–9.5, turbidity ≤4 NTU (at consumer's tap), Ni ≤0.02 mg/l, Pb ≤0.01 mg/l, and Fe ≤0.02 mg/l (Drinking Water Inspectorate

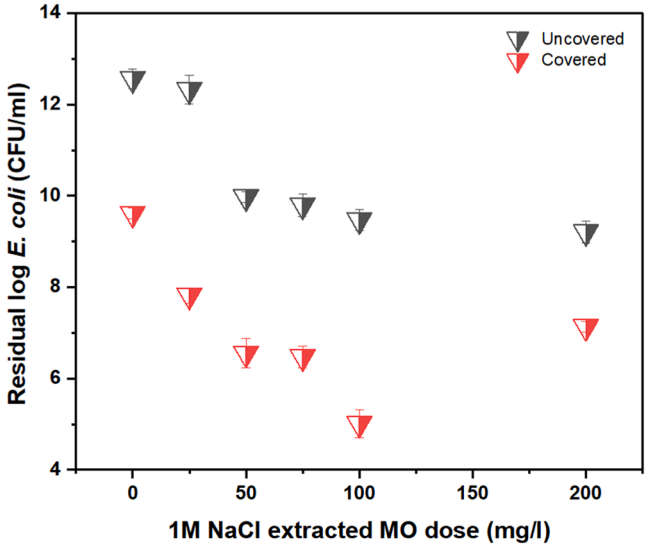


**Fig. 6.** Residual *E. coli* at different doses of MO salt extracted protein after 24 h of flocculation for covered and without cover beakers.

(DWI), 2016; World Health Organisation, 2022).

Initially, water treated with a 75 mg/l dose of MO exhibited promising results in reducing turbidity and *E. coli* levels post-flocculation. Subsequent filtration through a column containing sewage sludge biochar supported on a sand bed improved water quality. Overall, four scenarios of treating the contaminated water were explored: (a) MOSE, (b) sand, (c) biochar, and (d) a combination of MOSE, sand and biochar, as summarised in Table 8.

Of these scenarios, biochar treatment (scenario c) showed superior efficacy in reducing turbidity, heavy metals, and *E. coli* compared to sand treatment (scenario b). However, despite reducing turbidity to acceptable levels, biochar treatment left high concentrations of pathogens and heavy metals. In scenario d, where water was sequentially treated with MOSE, biochar, and sand, optimal results were achieved with a 6 cm bed height for both biochar and sand. This configuration resulted in clear water with minimal turbidity, reduced heavy metals concentrations, and the absence of *E. coli*. Moreover, slight increases in pH and levels of calcium and magnesium were observed, likely due to the mineral content of MO seeds.

As shown in Table 9, when MOSE was used solely, turbidity decreased from 200 NTU to nearly 4 NTU, which meets WHO standards. Despite a significant drop in *E. coli* levels from $1\times10^5$ CFU/ml to 150 CFU/ml, it fell short of drinking water criteria. Similarly, metal reduction was suboptimal. Biochar treatment (scenario c) outperformed sand (scenario b) in reducing turbidity, heavy metals, and *E. coli*. Despite achieving recommended turbidity levels, pathogens and metal concentrations remained high.

Scenario d involved initially treating contaminated water with 75 mg/l MO. Subsequently, the water was passed through a column filled with biochar and sand, each with bed heights of 4 cm, 6 cm, and 8 cm. Clearwater with less than 5 NTU turbidity was achieved with a bed height of 4 cm for both biochar and sand. However, some *E. coli* and lead (Pb) concentrations slightly exceeded recommended levels. Therefore, the bed height was increased to 6 cm for both biochar and sand. Clear water with 1.0 NTU turbidity and minimal Ni and Pb presence was obtained. Iron and silica levels were reduced, and no *E. coli* were detected. The pH level of the treated water rose slightly from 8.4 to 8.8 due to the alkaline nature of biochar. The increase in calcium and magnesium levels can be attributed to the mineral content of MO Lam. protein. Dissolved oxygen (DO) levels remained satisfactory between 7 and 7.5 mg/l, meeting UK and EPA criteria. While the WHO lacks specific guidance on DO levels, the UK and EPA standards range between 6 and 8.5 mg/l (World Health Organisation, 2022; D.W.I. dwi, 2019; E.P.A et al., 2014). The finally treated water met drinking water criteria according to WHO and UK standards. Notably, further increasing the bed height to 8 cm biochar and 8 cm sand did not significantly improve the quality of the treated water. The study's outcomes closely align with the predictions of hypothesis "b" while hypothesis "a" could not be verified.

#### 3.6.2. Optimum column dimensions

In each experimental condition, the flow rate of contaminated water passing through the bed remained constant at 32.14 ml /minute. Under the most effective operating parameters, both the biochar and sand within the column were set at a height of 6 cm. The biochar weighed 17 g, while the sand weighed 40 g, resulting in a column composition of 29.8 % biochar and 70.2 % sand by weight. To further understand the capacity of the column, the bed volume for both biochar and sand was calculated using Eq. (3) (Alchouron et al., 2021):

$$BV = \pi R^2 H \tag{3}$$

R represents the internal radius of the column containing biochar (1.25 cm), and H denotes the height of the adsorbent in the column (6 cm). Consequently, the bed volume was determined to be 29.43 $cm^3$. This calculation aids in assessing the column's capacity and efficiency in treating contaminated water under the specified conditions.

**Table 8**
Overview of water treatment scenarios a to d considered for comparison of different particle sizes of MO.

| Scenario | Treatment method | Particle-size |
|---|---|---|
| **a** | Moringa *oleifera* seed extract using a jar test flocculator | 0.4–0.8 mm |
| **b** | Contaminated water passed through a column packed with sand | 0.25–0.5 mm |
| **c** | Contaminated water passed through a column packed with biochar | 0.4–0.8 mm |
| **d** | Contaminated water pre-treated with MOSE passed through a column containing a combination of sand and biochar | - |

### 3.7. Mechanism of removal of contaminants

#### 3.7.1. Moringa oleifera

A chain of amino acids linked together by peptide bonds, called polypeptides, present in MO seed protein functions as a "coagulant" to remove contaminants such as turbidity, heavy metals and bacteria from water (Bichi et al., 2012; Okuda and Ali, 2019; Villaseñor-Basulto et al., 2018). These cationic proteins and peptides having a molecular mass of 3 – 60 kDa function actively when the pH of the solution is 6 – 10 (Vega Andrade et al., 2021). In this study, the pH of synthetic water was near 7 (neutral), and the seed protein was extracted in brine solution for enhanced solubility. Hence, effective coagulation was achieved. As the MO seed protein was added in the appropriate dose, the cationic proteins acted as charged polyelectrolytes, attracting the negatively charged *E. coli* and kaolin particles (added to create synthetic turbidity). Hence, the particles in a stable solution formed a colloid, initiating the coagulation mechanism in the beakers having MO seed protein. The stirring process (using the jar test flocculator) aided the formation of flocs. On becoming heavier, these flocs settled down under gravity, and the pure water was decanted. Hence, a substantial reduction in turbidity and *E. coli* concentration was noted after the MO treatment (Okuda and Ali, 2019; Fouad et al., 2019).

Another factor that supports coagulation is as the surface charges on the contaminant particles neutralise, the electrical double layer (EDL) surrounding the charges thickens. Thus, the particles come close to each other and are held together in a colloid through van der Waals forces (Chowdareddy et al., 2023; Shah et al., 2024a). The process is summarised in Fig. 7. It's worth noting that the presence of various functional groups like ketones, esters, carboxyl and anhydrides on the surface of the seed protein provide various sites to adsorb the contaminants and form inter-particle bridges (Shamsnejati et al., 2015b).

#### 3.7.2. Sewage sludge biochar (SSB)

This study showed a promising reduction in turbidity, *E. coli* and heavy metals using biochar. The primary mechanism for the removal of these contaminants is adsorption. The SEM analysis shown in Fig. 2, revealed that the biochar (SSB) possesses a large surface area due to pores on its surface. These pores play a crucial role in the adsorption process, allowing the biochar to capture contaminants such as kaolin particles, *E. coli*, Ni, and Pb, depending on the size and distribution of the pores (Li et al., 2017; Norberto et al., 2023). The adsorption process here is primarily driven by diffusion, where the concentration gradient between the contaminated water, which contains high levels of suspended kaolin particles, bacteria, and heavy metals, and the carbon-rich matrix of the SSB, facilitates the flow of pollutants into the biochar (Dharmarathna and Priyantha, 2024). Additionally, hydrophobic interactions support the adsorption process where heavy metals in the water engage in electron exchange with the SSB surface through the dissociation of acidic or anionic groups on the biochar (Shah et al., 2024a).

Electrostatic interactions also play a significant role in the adsorption

**Table 9**
A comparison of the removal of turbidity, heavy metals (Pb and Ni), and *E. coli* using MO, sand, and biochar individually and in combination at variable bed heights and settling times.

| Parameter | Contaminated water | Scenario a | Scenario b | Scenario c | Scenario d | | |
|---|---|---|---|---|---|---|---|
| | | MO (75 mg/l) | Sand (80 g) | Biochar (34 g) | Water treated with MO (75 mg/l) passed through a bed of biochar and sand | | |
| | | 2 h settling time | 12 cm bed height | 12 cm bed height | 4 cm bed height each | 6 cm bed height each | 8 cm bed height each |
| **pH** | 8.42 | 8.33 | 9.23 | 8.60 | 8.82 | 8.87 | 8.96 |
| **Appearance** | Very turbid | Moderately clear | Slightly turbid | Moderately Clear | Clear | Very clear | Very clear |
| **Turbidity (NTU)** | 200 | 4.28 | 5.7 | 4.42 | 2.93 | 1.0 | < 1 |
| **Ni (mg/L)** | 10 | 2.52 | 0.99 | 0.78 | 0.06 | 0.03 | 0.02 |
| **Pb (mg/L)** | 10 | 0.19 | 0.63 | 0.51 | 0.06 | 0.01 | 0.01 |
| ***E. coli* (CFU/ml)** | $1\times10^5$ | 150 | 750 | 650 | 50 | Not Detected | Not Detected |
| **Ca (mg/l)** | 36.05 | 42 | 26.58 | 59.68 | 55.20 | 59.64 | 61.53 |
| **Mg (mg/l)** | 6.62 | 10.23 | 5.93 | 35.12 | 46.50 | 50.33 | 52.52 |
| **Fe (mg/l)** | 0.04 | 0.06 | 0.04 | 0.02 | 0.03 | 0.01 | 0.01 |
| **$SiO_2$ (mg/l)** | 5.81 | 4.91 | 8.96 | 3.10 | 5.0 | 4.08 | 3.72 |

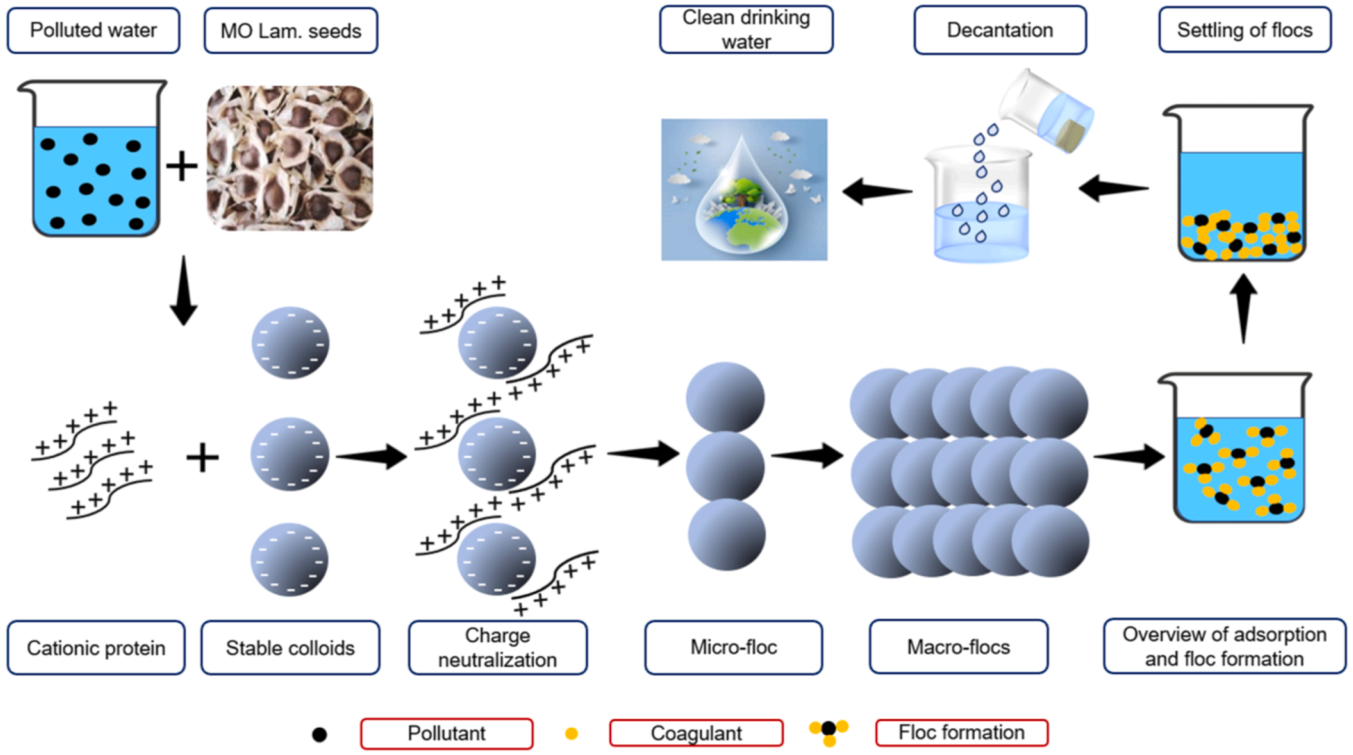


**Fig. 7.** Mechanism of the removal of contaminants from the contaminated water using MO seeds.

of Ni and Pb, as revealed by FTIR analysis informed by Fig. 1. The presence of hydroxyl, carboxylic, and carbonyl groups on the SSB surface, which are negatively charged, attracts the cationic metals, facilitating their binding to these functional groups. Conversely, positively charged functional groups, such as the amino group ($NH_2$), can attract and bind negatively charged contaminants (Zohaib Abbas, 2024). Hydrogen bonding further enhances the stability of the adsorbed contaminants, with functional groups like hydroxyl, carboxylic, and carbonyl forming hydrogen bonds with metal ions and *E. coli* on the SSB surface. These bonds prevent the desorption of the contaminants, ensuring their retention on the biochar surface, contributing to the overall effectiveness of the adsorption process (Li et al., 2017).

### 3.8. Implications, scalability and economic feasibility

The study offers a potential route for removing heavy metals and pathogens from drinking water using *Moringa oleifera* Lam. seeds, sand, and biochar on a domestic scale. MO trees are widely cultivated in African and Asian regions, where the proposed system can offer a cost-effective way of treating water. The methodology demonstrated in this study to extract MO seed protein can be implemented at a household level through dehusking MO seeds. The coagulant protein in the MO seeds can then be extracted using table salt as a solvent. Biochar can be obtained from any carbon-rich material, such as waste crops, dead leaves, or sewage sludge. The global availability of sand further enhances the scalability of the proposed methodology. Although none of the clarifiers individually produced clean water, the combined use of

MO seeds, sand, and biochar has demonstrated to successfully remove all the toxicants to WHO-acceptable levels. Consequently, the procedure can be replicated domestically to obtain clean drinking water, particularly in underprivileged and disaster-affected regions.

### 3.9. Cost analysis

The treatment cost will depend on the quantity of water to be treated, the concentration and nature of contaminants present, and the degree of purity required. Below is a cost analysis of the process based on treating 100 L of highly contaminated water with 200 NTU turbidity, 10 mg/L of each Ni and Pb as representative heavy metals, and $1\times10^5$ CFU/ml *E. coli* concentration. The optimum dose of MO, according to the study results, is 75 mg/L. So, the amount of MO seed powder required to treat 100 L water is 7500 mg or 7.5 g. The weight of the seeds (Shelled) will almost be 1.5 times, i.e. 11.2 g (Jahn, 1986). The amount of biochar required = 17 g (Section 3.6.2) x 100 = 1700 g = 1.7 kg. The actual amount of biochar required = calculated amount/ cycles of use = 1.7/3 = 0.56 kg.

Moving on to the cost of the materials used, the cost of MO seeds (Herbyzone, Lahore, Pakistan) is £5/1000 g. This translates into 5.6 pence for 11.2 g seeds. The cost of commercially produced biochar is £1/kg (Carbon Gold, 2024). Hence, the cost of 0.56 kg of biochar is £0.56 or 56 pence. The cost of materials (MO seeds and biochar) required to treat 100 L of contaminated water is 56.56 pence, which translates into 0.56 pence/ L. Further experiments and scale-up efforts are needed to bridge the gap between laboratory findings and practical applications.

### 3.10. Comparing MO and biochar with conventional and emerging technologies

Several physical, chemical, and biological methods may be used to remove contaminants from water, depending on the economic constraints, the nature and concentration of contaminants, and the technology available (Binnie Chris Thomas, 2018; Kausley et al., 2019; WHO, 2018). The conventional methods include screening, filtration, aeration, straining, sedimentation, and filtration. These methods primarily remove suspended solids (Talpur and Talpur, 2018; Ministry of Health Malaysia, 2018). Coagulation removes dissolved solids as well, to a certain extent. Coagulants generally used include aluminium sulphate (alum) and ferric chloride. The drawbacks of using these chemicals include the formation of voluminous sludge, health impacts such as the association of neurotoxic and neurodegenerative diseases like Alzheimer's and their limited efficacy for cold water (Muhammad et al., 2015; Amran et al., 2018b; Megersa et al., 2019; Ndabigengesere and Subba Narasiah, 1998; Adesina et al., 2019). Other methods used to extract contaminants, including heavy metals, are precipitation, ion exchange, and filtration using packed beds, adsorbents such as activated carbon, and dendritic-based polymers (Sajid et al., 2018). Membrane-based processes like reverse osmosis (RO), microfiltration, ultrafiltration (Kausley et al., 2019) and electrochemical methods, including electro-coagulation, electro-oxidation and electro-dialysis, can effectively remove both anions and cations from water (Colin Ingram, 2006). The systems based on solar energy are also being effectively used (Ahmed, 2024; Zeeshan et al., 2023; Alao et al., 2023b). However, these systems are expensive to install and maintain, requiring skilled labour. The use of chemical coagulants also causes various health-related problems, as discussed. These demerits justify introducing cost-effective, sustainable, and environmentally friendly methods to treat water based on green chemistry.

### 3.11. Limitations and future directions

The research faced certain limitations, including the inability to perform post-treatment FTIR analysis on *Moringa oleifera* protein due to technical constraints related to high dilution levels. This limitation prevented the complete characterisation of the surface functionalities involved in contaminant adsorption. Additionally, while the study demonstrated the effectiveness of biochar, sand, and *Moringa oleifera* in removing contaminelectrochemical methods, including elecants, the varying levels of success across different materials and contaminants highlight the complexity of optimising these adsorbents for real-world applications. Future research should focus on refining the characterisation techniques, exploring alternative methods for evaluating diluted samples, and further investigating the adsorption mechanisms to enhance the efficacy of these materials. Moreover, there is a need for extended studies to test the long-term stability and regeneration potential of these adsorbents in varying environmental conditions.

## 4. Conclusions

The research aimed to purify drinking water using sustainable resources, specifically MO Lam., sand, and biochar, to remove contaminants like turbidity, heavy metals, and *E. coli*. Synthetically contaminated water was first treated with MO seed protein extracted in a 1 M NaCl solution. The coagulant protein was thoroughly mixed into the contaminated water using a jar test flocculator. After a 2 h settling time, the optimum MO seed dose of 75 mg/l reduced the water turbidity from 200 NTU to < 5 NTU, achieving a 90–99 % reduction in *E. coli*. However, no significant decrease in the concentration of heavy metals (Ni and Pb) was noted. This water was then passed through a column containing biochar and sand (30 % and 70 % by weight, respectively). At an optimum bed height of 12 cm (6 cm for each adsorbent), clear water of 1 NTU was obtained. Both heavy metals were removed to acceptable levels, and no residual *E. coli* was detected. The treated water was further evaluated for other parameters such as pH, calcium, magnesium, silica and iron levels, all meeting WHO and UK criteria for safe drinking water. Although promising results were obtained, further experiments and scale-ups are necessary to bridge the gap between laboratory scale results and practical applications.

## CRediT authorship contribution statement

**Ahsan Abbas Shah:** Writing – review & editing, Writing – original draft, Visualization, Validation, Software, Methodology, Investigation, Formal analysis, Data curation, Conceptualization. **Arun Arjunan:** Writing – review & editing, Writing – original draft, Validation, Supervision, Methodology, Funding acquisition, Formal analysis, Conceptualization. **Georgina Manning:** Writing – review & editing, Validation, Supervision, Methodology, Funding acquisition, Formal analysis, Conceptualization. **Maryam Batool:** Writing – review & editing, Writing – original draft, Validation, Supervision, Software, Methodology, Investigation, Formal analysis, Conceptualization. **Julia Zakharova:** Writing – review & editing, Visualization, Supervision, Methodology, Funding acquisition, Formal analysis, Conceptualization. **Alisha J. Hawkins:** Writing – review & editing, Validation, Software, Investigation, Formal analysis. **Fatima Ajani:** Writing – review & editing, Validation, Software, Methodology, Investigation, Formal analysis. **Ioanna Androulaki:** Writing – review & editing, Visualization, Validation, Software, Methodology, Investigation, Formal analysis. **Anusha Thumma:** Writing – review & editing, Validation, Software, Methodology, Investigation, Formal analysis.

## Declaration of Competing Interest

All authors whose names are listed immediately below certify that they have NO affiliations with or involvement in any organisation or entity with any financial interest (such as honoraria; educational grants; participation in speakers' bureaus; membership, employment, consultancies, stock ownership, or other equity interest; and expert testimony or patent-licensing arrangements), or non-financial interest (such as personal or professional relationships, affiliations, knowledge or beliefs)

in the subject matter or materials discussed in this manuscript.

## Acknowledgements

The authors thank Paul Bates, Diane Spencer, Keith Holding, Surila Darbar, David Townrow, Andrew Brook, Baljinder Singh, Andrew Gould, and David Luckhurst from the University of Wolverhampton for their generous technical support throughout this study.

## Data availability

Data will be made available on request.

## References

Z. Abbas, I. Shahid, S. Ali, M. Naseer, M.A. Khalid, S. Tabraiz, I. Zaheer, M. Zeeshan, Graphene and graphene oxide-based nanomaterials as a promising tool for the mitigation of heavy metals from water and wastewater, 2023: pp. 197–222. ⟨https://doi.org/10.1201/9781003326281-12⟩.

Adesina, O.A., Abdulkareem, F., Yusuff, A.S., Lala, M., Okewale, A., 2019. Response surface methodology approach to optimization of process parameter for coagulation process of surface water using Moringa oleifera seed. S Afr. J. Chem. Eng. 28, 46–51. https://doi.org/10.1016/j.sajce.2019.02.002.

ADWG, Australian Drinking Water Guidelines, (2024). ⟨https://www.nhmrc.gov.au/about-us/publications/australian-drinking-water-guidelines#block-views-block-file-attachments-content-block-1⟩ (accessed August 22, 2024).

Ahmed, Y.E., 2024. Intelligent watering by using solar energy system. Babylon. J. Internet Things 2024, 53–59. https://doi.org/10.58496/bjiot/2024/007.

Alao, J.O., Fahad, A., Abdo, H.G., Ayejoto, D.A., Almohamad, H., Ahmad, M.S., Nur, M. S., Danjuma, T.T., Yusuf, M.A., Francis, O.T., Joy, A.O., 2023b. Effects of dumpsite leachate plumes on surface and groundwater and the possible public health risks. Sci. Total Environ. 897, 165469. https://doi.org/10.1016/j.scitotenv.2023.165469.

Alao, J.O., Abdo, H.G., Ayejoto, D.A., Mohammed, M.A.A., Danladi, E., Saqr, A.M., Almohamad, H., Fahad, A., 2023a. Evaluation of groundwater contamination and the health risk due to landfills using integrated geophysical methods and Physiochemical Water Analysis. Case Stud. Chem. Environ. Eng. 8. https://doi.org/10.1016/j.cscee.2023.100523.

Alchouron, J., Navarathna, C., Rodrigo, P.M., Snyder, A., Chludil, H.D., Vega, A.S., Bosi, G., Perez, F., Mohan, D., Pittman, C.U., Mlsna, T.E., 2021. Household arsenic contaminated water treatment employing iron oxide/bamboo biochar composite: An approach to technology transfer. J. Colloid Interface Sci. 587, 767–779. https://doi.org/10.1016/j.jcis.2020.11.036.

Amran, A.H., Zaidi, N.S., Muda, K., Loan, L.W., 2018b. Effectiveness of natural coagulant in coagulation process: A review. Int. J. Eng. Technol. 7, 34–37. https://doi.org/10.14419/ijet.v7i3.9.15269.

Amran, A.H., Zaidi, N.S., Muda, K., Loan, L.W., 2018a. Effectiveness of natural coagulant in coagulation process: A review. Int. J. Eng. Technol. 7, 34–37. https://doi.org/10.14419/ijet.v7i3.9.15269.

Amran, T., Mohd, T., Bohairah, N.A., Jaafar, M.Z., 2022. Characterization of quartz sand as an adsorbent for anionic surfactant adsorption with presences of alkaline and polymer. Chem. Eng. Trans. 95, 283–288. https://doi.org/10.3303/CET2295048.

Ayejoto, D.A., Egbueri, J.C., 2023. Human health risk assessment of nitrate and heavy metals in urban groundwater in Southeast Nigeria. Acta Ecol. Sin. https://doi.org/10.1016/j.chnaes.2023.06.008.

Ayejoto, D.A., Agbasi, J.C., Nwazelibe, V.E., Egbueri, J.C., Alao, J.O., 2023. Understanding the connections between climate change, air pollution, and human health in Africa: insights from a literature review. J. Environ. Sci. Health C. Toxicol. Carcinog. 41, 77–120. https://doi.org/10.1080/26896583.2023.2267332.

Ayejoto, D.A., Agbasi, J.C., Egbueri, J.C., Echefu, K.I., 2024. Assessment of oral and dermal health risk exposures associated with contaminated water resources: an update in Ojoto area, southeast Nigeria. Int J. Environ. Anal. Chem. 104, 641–661. https://doi.org/10.1080/03067319.2021.2023515.

Ayeni, E.A., Aldossary, A.M., Ayejoto, D.A., Gbadegesin, L.A., Alshehri, A.A., Alfassam, H.A., Afewerky, H.K., Almughem, F.A., Bello, S.M., Tawfik, E.A., 2022. Neurodegenerative diseases: implications of environmental and climatic influences on neurotransmitters and neuronal hormones activities. Int J. Environ. Res Public Health 19. https://doi.org/10.3390/ijerph191912495.

Azhar-ul-Haq, M., Javed, T., Abid, M.A., Masood, H.T., Muslim, N., 2022. Adsorptive removal of hazardous crystal violet dye onto banana peel powder: equilibrium, kinetic and thermodynamic studies. J. Dispers. Sci. Technol. 1–16. https://doi.org/10.1080/01932691.2022.2158851.

Babakhani, A., Sartaj, M., 2023. Optimization of nickel(II) adsorption by sodium tripolyphosphate crosslinked chitosan using response surface methodology (RSM). Sustain. Chem. Environ. 2. https://doi.org/10.1016/j.scenv.2023.100019.

Barbosa, A.D., da Silva, L.F., de Paula, H.M., Romualdo, L.L., Sadoyama, G., Andrade, L. S., 2018. Combined use of coagulation (M. oleifera) and electrochemical techniques in the treatment of industrial paint wastewater for reuse and/or disposal. Water Res 145, 153–161. https://doi.org/10.1016/j.watres.2018.08.022.

Baskaran, P., Abraham, M., 2022. Evaluation of groundwater quality and heavy metal pollution index of the industrial area, Chennai. Phys. Chem. Earth 128. https://doi.org/10.1016/j.pce.2022.103259.

Bichi, M.H., Agunwamba, J.C., Muyibi, S.A., 2012. Kinetics of water disinfection with Moringa oleifera seeds extract. J. Environ. Earth Sci. 2, 58–68. ⟨http://irep.iium.edu.my/25910/⟩.

Binnie, C.T., Kimber, M., 2018.Basic Water Treatment, 6th ed. London.

Blanco-Canqui, H., 2019. Biochar and water quality. J. Environ. Qual. 48, 2–15. https://doi.org/10.2134/jeq2018.06.0248.

Carbon Gold, 2024. Biochar UK, Usage of Biochar.

Cha, J.S., Park, S.H., Jung, S.C., Ryu, C., Jeon, J.K., Shin, M.C., Park, Y.K., 2016. Production and utilization of biochar: a review. J. Ind. Eng. Chem. 40, 1–15. https://doi.org/10.1016/j.jiec.2016.06.002.

Chowdareddy, S., Rajesh, C., Rajashekara, R., Nagaraju, P., 2023. Moringa oleifera: a sustainable method to treat fluoride-contaminated water. Water Supply 23, 615–623. https://doi.org/10.2166/WS.2023.025.

Colin Ingram, 2006. The Drinking Water Book, 2nd ed. Crown Publishing, New York.

Cotruvo, J.A., 2017. 2017 Who guidelines for drinking water quality: first addendum to the fourth edition. J. Am. Water Works Assoc. 109, 44–51. https://doi.org/10.5942/jawwa.2017.109.0087.

D.W.I., 2019. Drinking water annual report. ⟨https://www.dwi.gov.uk/what-we-do/annual-report/drinking-water-2019/⟩.

Dandesa, B., Akuma, D.A., Alemayehu, E., 2023. Water purification improvement using Moringa oleifera seed extract pastes for coagulation follow scoria filtration. Heliyon 9. https://doi.org/10.1016/j.heliyon.2023.e17420.

De Paula, H.M., De Oliveira Ilha, M.S., Andrade, L.S., 2014. Concrete plant wastewater treatment process by coagulation combining aluminum sulfate and Moringa oleifera powder. J. Clean. Prod. 76, 125–130. https://doi.org/10.1016/j.jclepro.2014.04.031.

Delelegn, A., Sahile, S., Husen, A., 2018. Water purification and antibacterial efficacy of Moringa oleifera Lam. Agric. Food Secur 7, 1–10. https://doi.org/10.1186/s40066-018-0177-1.

Dharmarathna, S.P., Priyantha, N., 2024. Investigation of boundary layer effect of intra-particle diffusion on methylene blue adsorption on activated carbon. Energy Nexus 14. https://doi.org/10.1016/j.nexus.2024.100294.

Doll, R., 1993. Review: Alzheimer's disease and environmental aluminium. Age Ageing 22, 138–153. https://doi.org/10.1093/ageing/22.2.138.

Drinking Water Inspectorate (DWI), 2016. Guidelines for drinking water quality (UK).

E.P. A, Drinking Water Parameters, Environmental Protection Agency, 2014. wwwepa.ie. 1–9. .

Fouad, E.A., Abu Elnaga, A.S.M., Kandil, M.M., 2019. Antibacterial efficacy of Moringa oleifera leaf extract against pyogenic bacteria isolated from a dromedary camel (Camelus dromedarius) abscess. Vet. World 12, 802–808. https://doi.org/10.14202/vetworld.2019.802-808.

Gaikwad, V.T., Munavalli, G.R., 2019. Turbidity removal by conventional and ballasted coagulation with natural coagulants. Appl. Water Sci. 9, 1–9. https://doi.org/10.1007/s13201-019-1009-6.

Ghzal, Q., Javed, T., Batool, M., 2023. Potential of easily prepared low-cost rice husk biochar and burnt clay composite for the removal of methylene blue dye from contaminated water. Environ. Sci. 9, 2925–2941. https://doi.org/10.1039/d3ew00392b.

Grabow, S.J.L., Morgan, W.O.K., G, W.S., Jahn, S.A., 1985. Toxicity and mutagenicity evaluation of water coagulated with Moringa oleifera seed preparations using fish, protozoan, bacterial, coliphage, enzyme, and Ames Salmonella assays. Water SA 11.

Hoa, N.T., Hue, C.T., 2018. Enhanced water treatment by Moringa oleifera seeds extract as the bio-coagulant: Role of the extraction method. J. Water Supply. Res. Technol. 67, 634–647. https://doi.org/10.2166/aqua.2018.070.

Huggins, T.M., Haeger, A., Biffinger, J.C., Ren, Z.J., 2016. Granular biochar compared with activated carbon for wastewater treatment and resource recovery. Water Res. 94, 225–232. https://doi.org/10.1016/j.watres.2016.02.059.

Inyang, X., Gao, M.I., Yao, B., Xue, Y., Zimmerman, Y., Mosa, A., Pullammanappallil, A., Ok, P., Cao, Y.S., 2016. A review of biochar as a low-cost adsorbent for aqueous heavy metal removal. Crit. Rev. Environ. Sci. Technol. 406–433.

Iqbal, A., Cevik, E., Mustafa, A., Qahtan, T.F., Zeeshan, M., Bozkurt, A., 2024. Emerging developments in polymeric nanocomposite membrane-based filtration for water purification: a concise overview of toxic metal removal. Chem. Eng. J. 481. https://doi.org/10.1016/j.cej.2024.148760.

Jahn, SamiaAlazharia, 1986. Proper Use of African natural coagulants for rural water supplies, 1st ed. Deutsche Gesellschaft Federal Republic of Germany.

Johannes Lehmann, S.J., 2015. Biochar for Environmental Management: Science, Technology and Implementation. Taylor & Francis.

Kausley, S.B., Dastane, G.G., Kumar, J.K., Desai, K.S., Doltade, S.B., Pandit, A.B., 2019a. Clean Water for Developing Countries: Feasibility of Different Treatment Solutions, 2nd ed. Elsevier Inc. https://doi.org/10.1016/B978-0-12-409548-9.11079-6.

Kozyatnyk, I., Njenga, M., 2023. Use of biochar and Moringa oleifera in greywater treatment to remove heavy metals and contaminants of emerging concern. Bioresour. Technol. Rep. 24. https://doi.org/10.1016/j.biteb.2023.101615.

Kwabena Ntibrey, R.A., Kuranchie, F.A., Gyasi, S.F., 2020. Antimicrobial and coagulation potential of Moringa oleifera seed powder coupled with sand filtration for treatment of bath wastewater from public senior high schools in Ghana. Heliyon 6, e04627. https://doi.org/10.1016/j.heliyon.2020.e04627.

L, (LE), Y.E., 2020. Water Quality Standards; European water quality standards.

Lau, A.Y.T., Tsang, D.C.W., Graham, N.J.D., Ok, Y.S., Yang, X., Li, X. dong, 2017. Surface-modified biochar in a bioretention system for Escherichia coli removal from stormwater. Chemosphere 169, 89–98. https://doi.org/10.1016/j.chemosphere.2016.11.048.

Li, H., Dong, X., da Silva, E.B., de Oliveira, L.M., Chen, Y., Ma, L.Q., 2017. Mechanisms of metal sorption by biochars: biochar characteristics and modifications. Chemosphere 178, 466–478. https://doi.org/10.1016/j.chemosphere.2017.03.072.

Madsen, M., Schlundt, J., Omer, E.F.E., 1987. Effect of water coagulation by seeds of Moringa oleifera on bacterial concentrations. J. Trop. Med. Hyg. 90, 101–109. https://doi.org/10.1016/0378-8741(88)90285-1.
Mandu, B.G., Inyang Ying, I., Yao, Yingwen, Xue, Andrew, Zimmerman, Ahmed, Mosa Pratap, Pullammanappallil, Ok, Yong Sik, Xinde, Cao, et al., 2015. Biochar as an absorbent for heavy metal removal. Crit. Rev. Environ. Sci. Technol. 113–139.
Megersa, M., Gach, W., Beyene, A., Ambelu, A., Triest, L., 2019. Effect of salt solutions on coagulation performance of Moringa stenopetala and Maerua subcordata for turbid water treatment. Sep Purif. Technol. 221, 319–324. https://doi.org/10.1016/j.seppur.2019.04.013.
Ministry of Health Malaysia, 2018. National standard for organics. Beehive.
Mohanty, S.K., Cantrell, K.B., Nelson, K.L., Boehm, A.B., 2014. Efficacy of biochar to remove Escherichia coli from stormwater under steady and intermittent flow. Water Res. 61, 288–296. https://doi.org/10.1016/j.watres.2014.05.026.
Mortula, M., Bard, S.M., Walsh, M.E., Gagnon, G.A., 2009. Aluminum toxicity and ecological risk assessment of dried alum residual into surface water disposal. Can. J. Civ. Eng. 36, 127–136. https://doi.org/10.1139/S08-042.
Muhammad, I.M., Abdulsalam, S., Abdulkarim, A., Bello, A.A., 2015. Water melon seed as a potential coagulant for water treatment. Global J. Res. Eng.: C. Chem. Eng. 15, 17–24.
Muneer, I., Javed, T., Majeed, A.Abdul, Masood, H.T., 2021. A brief study of adsorption of Congo red dye over saw dust of Cedrus deodara. Desalin. Water Treat. 235, 272–282. https://doi.org/10.5004/dwt.2021.27596.
Ndabigengesere, A., Subba Narasiah, K., 1998. Quality of water treated by coagulation using Moringa oleifera seeds. Water Res. 32, 781–791. https://doi.org/10.1016/S0043-1354(97)00295-9.
Ndabigengesere, A., Narasiah, K.S., Talbot, B.G., 1995. Active agents and mechanism of coagulation of turbid waters using Moringa oleifera. Water Res 29, 703–710. https://doi.org/10.1016/0043-1354(94)00161-Y.
Nkhata, D., 2002. Moringa as an alternative to aluminium sulphate, people and systems for water, sanitation and health. Proc. 27th WEDC Conf. 494–496.
Norberto, J., Zoroufchi Benis, K., McPhedran, K.N., Soltan, J., 2023. Microwave activated and iron engineered biochar for arsenic adsorption: life cycle assessment and cost analysis. J. Environ. Chem. Eng. 11. https://doi.org/10.1016/j.jece.2023.109904.
Okuda, T., Ali, E.N., 2019. Application of Moringa oleifera plant in water treatment. Energy Environ. Sustain. 63–79. https://doi.org/10.1007/978-981-13-3259-3_4.
Okuda, T., Baes, A.U., Nishijima, W., Okada, M., 1999. Improvement of extraction method of coagulation active components from Moringa oleifera seed. Water Res. 33, 3373–3378. https://doi.org/10.1016/S0043-1354(99)00046-9.
Sajid, M., Nazal, M.K., Ihsanullah, Baig, N., Osman, A.M., 2018. Removal of heavy metals and organic pollutants from water using dendritic polymers based adsorbents: a critical review. Sep. Purif. Technol. 191, 400–423. https://doi.org/10.1016/j.seppur.2017.09.011.
Saleem, M., Bachmann, R.T., 2019. A contemporary review on plant-based coagulants for applications in water treatment. J. Ind. Eng. Chem. 72, 281–297. https://doi.org/10.1016/j.jiec.2018.12.029.
Saleem, M., Sami, A.J., Bachmann, R.T., 2020. Characterisation and Coagulant Activity Screening of Fractionated Water-soluble Seed Proteins From Moringa oleifera. In: Mater Today Proc. Elsevier Ltd, pp. 207–210. https://doi.org/10.1016/j.matpr.2020.03.700.
Sera, P.R., Diagboya, P.N., Akpotu, S.O., Mtunzi, F.M., Chokwe, T.B., 2021. Potential of valourized Moringa oleifera seed waste modified with activated carbon for toxic metals decontamination in conventional water treatment. Bioresour. Technol. Rep. 16. https://doi.org/10.1016/j.biteb.2021.100881.
Shabaa, G.J., Al-Jboory, W.S.H., Sabre, H.M., Alazmi, A., Kareem, M.M., AlKhayyat, A., 2021. Plant-based coagulants for water treatment. IOP Conf. Ser. Mater. Sci. Eng. 1058, 12001. https://doi.org/10.1088/1757-899x/1058/1/012001.
Shah, A., Arjunan, A., Baroutaji, A., Zakharova, J., 2023. A review of physicochemical and biological contaminants in drinking water and their impacts on human health. Water Sci. Eng. https://doi.org/10.1016/j.wse.2023.04.003.
Shah, A., Zakharova, J., Batool, M., Coley, M.P., Arjunan, A., Hawkins, A.J., Bolarinwa, T., Devi, S., Thumma, A., Williams, C., 2024b. Removal of cadmium and zinc from water using sewage sludge-derived biochar. Sustain. Chem. Environ. 6, 100118. https://doi.org/10.1016/j.scenv.2024.100118.
Shah, A., Arjunan, A., Manning, G., Zakharova, J., Andraulaki, I., Batool, M., 2024a. The effect of dose, settling time, shelf life, storage temperature and extractant on Moringa oleifera Lam. protein coagulation efficiency. Environ. Nanotechnol. Monit. Manag. 21. https://doi.org/10.1016/j.enmm.2024.100919.
Shah, A., Arjunan, A., Thumma, A., Zakharova, J., Bolarinwa, T., Devi, S., Batool, M., 2024a. Adsorptive removal of arsenic from drinking water using KOH-modified sewage sludge-derived biochar. Clean. Water 2, 100022. https://doi.org/10.1016/j.clwat.2024.100022.
Shah, A., Manning, G., Zakharova, J., Arjunan, A., Batool, M., Hawkins, A.J., Androulaki, I., 2024c. Particle size effect of Moringa oleifera Lam. seeds on the turbidity removal and antibacterial activity for drinking water treatment. Environ. Chem. Ecotoxicol. https://doi.org/10.1016/j.enceco.2024.07.008.
Shakoor, M.B., Ali, S., Rizwan, M., Abbas, F., Bibi, I., Riaz, M., Khalil, U., Niazi, N.K., Rinklebe, J., 2020. A review of biochar-based sorbents for separation of heavy metals from water. Int J. Phytoremediat. 22, 111–126. https://doi.org/10.1080/15226514.2019.1647405.
Shamsnejati, S., Chaibakhsh, N., Pendashteh, A.R., Hayeripour, S., 2015b. Mucilaginous seed of Ocimum basilicum as a natural coagulant for textile wastewater treatment. Ind. Crops Prod. 69, 40–47. https://doi.org/10.1016/j.indcrop.2015.01.045.
Shamsnejati, S., Chaibakhsh, N., Pendashteh, A.R., Hayeripour, S., 2015a. Mucilaginous seed of Ocimum basilicum as a natural coagulant for textile wastewater treatment. Ind. Crops Prod. 69, 40–47. https://doi.org/10.1016/j.indcrop.2015.01.045.
Sizmur, T., Fresno, T., Akgül, G., Frost, H., Moreno-Jiménez, E., 2017. Biochar modification to enhance sorption of inorganics from water. Bioresour. Technol. 246, 34–47. https://doi.org/10.1016/j.biortech.2017.07.082.
Su, Y., Wen, Y., Yang, W., Zhang, X., Xia, M., Zhou, N., Xiong, Y., Zhou, Z., 2021. The mechanism transformation of ramie biochar's cadmium adsorption by aging. Bioresour. Technol. 330, 124947. https://doi.org/10.1016/j.biortech.2021.124947.
Tabraiz, S., Nasreen, S., Qureshi, L.A., Zeeshan, M., Ahmad, I., Ahmed, S., Hassan, Z., 2016. Sewage land disposal and unpaved drains: threat to groundwater quality. Desalin. Water Treat. 57, 20464–20469. https://doi.org/10.1080/19443994.2015.1110723.
Talpur, H.A., Talpur, S.A., 2018. Physio-chemical assessment of water sources for drinking purpose in Badin City, Sindh Province, Pakistan, (Water Supply Schemes and Hand Pumps). Res. Gate.
U. Nations, 2017. Sustainable Development Goals. ⟨https://www.un.org/sustainabledevelopment/sustainable-development-goals/⟩.
U.S.E.P.A. (EPA), 2018. 2018 Edition of the drinking water standards and health advisories tables. ⟨http://wwwepa.gov/sites/production/files/2018-03/documents/dwtable2018.pdf⟩.
Ueda Yamaguchi, N., Cusioli, L.F., Quesada, H.B., Camargo Ferreira, M.E., Fagundes-Klen, M.R., Salcedo Vieira, A.M., Gomes, R.G., Vieira, M.F., Bergamasco, R., 2021. A review of Moringa oleifera seeds in water treatment: trends and future challenges. Process Saf. Environ. Prot. 147, 405–420. https://doi.org/10.1016/j.psep.2020.09.044.
UK Biochar Research Centre | Welcome to the UKBRC, (n.d.). ⟨https://www.biochar.ac.uk/index.php⟩ (accessed April 13, 2021).
UNDP, 2023. Sustainable Development Goals.
Vega Andrade, P., Palanca, C.F., de Oliveira, M.A.C., Ito, C.Y.K., dos Reis, A.G., 2021. Use of Moringa oleifera seed as a natural coagulant in domestic wastewater tertiary treatment: physicochemical, cytotoxicity and bacterial load evaluation. J. Water Process Eng. 40. https://doi.org/10.1016/j.jwpe.2020.101859.
Villaseñor-Basulto, D.L., Astudillo-Sánchez, P.D., del Real-Olvera, J., Bandala, E.R., 2018. Wastewater treatment using Moringa oleifera Lam seeds: a review. J. Water Process Eng. 23, 151–164. https://doi.org/10.1016/j.jwpe.2018.03.017.
Wang, X., Li, C., Li, Z., Yu, G., Wang, Y., 2019. Effect of pyrolysis temperature on characteristics, chemical speciation and risk evaluation of heavy metals in biochar derived from textile dyeing sludge. Ecotoxicol. Environ. Saf. 168, 45–52. https://doi.org/10.1016/j.ecoenv.2018.10.022.
Wei, D., Li, B., Huang, H., Luo, L., Zhang, J., Yang, Y., Guo, J., Tang, L., Zeng, G., Zhou, Y., 2018. Biochar-based functional materials in the purification of agricultural wastewater: fabrication, application and future research needs. Chemosphere 197, 165–180. https://doi.org/10.1016/j.chemosphere.2017.12.193.
WHO, 2018. Household Water Treatment and Safe Storage. Treatment Technologies. ⟨http://www.who.int/household_water/research/technologies_intro/en/⟩.
Wok Grabow, J.L.S., Morgan, W.S.G., Jahn, S.A.A., Grabow, , 1985. Easiest method toxicity evaluation of MO Seeds.PDF.
World Health Organisation, 2022. Fourth edition incorporating the first and second addenda Guidelines for drinking-water quality.
Yavuz, C.I., Vaizoğlu, S.A., Güler, Ç., 2013. Aluminium in drinking water. TAF Prev. Med. Bull. 12, 589–596. https://doi.org/10.5455/pmb.1-1345809534.
Zeeshan, M., Ruhl, A.S., 2023. Fates of potentially persistent and mobile organic substances in embedded outdoor columns for artificial groundwater recharge simulation. Water Res. 245. https://doi.org/10.1016/j.watres.2023.120615.
Zeeshan, M., Klitzke, S., Ruhl, A.S., 2023. Changes in dissolved organic matter and oxygen consumption in different bank filtration simulations at different scales. Environ. Sci. Water Res. Technol. 9, 1862–1869. https://doi.org/10.1039/D3EW00008G.
Zohaib Abbas, I.S.S.A.M.N.N.M.A.K.S.T.I.E.Z.M.Z., 2024. Graphene and graphene oxide-based nanomaterials as a promising tool for the mitigation of heavy metals from water and wastewater. In: Membrane Technologies for Heavy Metals Removal from Water, 1st ed. ImprintCRC Press, pp. 1–26.